ATMOSPHERIC SCIENCE LETTERS
*Atmos. Sci. Let.* (2014)
Published online in Wiley Online Library
(wileyonlinelibrary.com) **DOI:** 10.1002/asl2.492

RMetS
Royal Meteorological Society

# The influence of synoptic weather regimes on UK air quality: analysis of satellite column $NO_2$

R. J. Pope,[1]* N. H. Savage,[2] M. P. Chipperfield,[1] S. R. Arnold[1] and T. J. Osborn[3]

[1]*Institute for Climate and Atmospheric Science, School of Earth and Environment, University of Leeds, Leeds LS2 9JT, UK*
[2]*Met Office, Exeter EX1 3PB, UK*
[3]*Climatic Research Unit, School of Environmental Sciences, University of East Anglia, Norwich NR4 7TJ, UK*

**Correspondence to:*
*R. Pope, Institute for Climate and Atmospheric Science, School of Earth and Environment, University of Leeds, Leeds LS2 9JT, UK.*
*E-mail: eerjp@leeds.ac.uk*

Received: 9 October 2013
Revised: 13 December 2013
Accepted: 7 February 2014

## Abstract

**Groupings of Lamb weather types (LWTs) are used to assess the influence of synoptic meteorology on UK tropospheric column $NO_2$. Composite satellite maps using daily 2005–2011 data show significant $NO_2$ anomalies for each group. Hence, despite large day-to-day variability and significant uncertainty in individual retrievals, the satellite data can be used to determine national-scale column $NO_2$ variations under different meteorological conditions. Under cyclonic conditions, $NO_2$ is reduced, while anticyclonic conditions aid its accumulation, especially during winter, consistent with trapping of surface emissions and slower photochemical processing. This composite dataset can be used to test seasonal simulations of air quality models.**

**Keywords:** **Lamb weather type; OMI $NO_2$; air quality**

## 1. Introduction

Regional weather exerts a strong influence on local air quality (AQ) through aiding both the accumulation and dispersal of emitted pollutants, and controlling their transport on a regional scale. Models have been developed to predict AQ, but need to be evaluated against observations. Satellite data provide an important source of data for such evaluation, as demonstrated by Huijnen *et al.* (2010), and greater knowledge of such observations allows for enhanced model development (e.g. detection of an observational seasonal cycle can then improve model representation of such features). Here we analyse a long data record (2005–2011) of satellite tropospheric column $NO_2$ over the UK, to determine the influence of specific climatological patterns of meteorology on regional $NO_2$ distributions.

Lamb weather types (LWTs) provide a useful tool to classify synoptic meteorology over the UK (Jones *et al.*, 2013). They are an objective description of the daily midday atmospheric circulation over the UK based on mean sea level pressure reanalysis data. Many studies have investigated the link between surface observations of atmospheric chemistry and synoptic meteorology by using LWTs. For example, Davies *et al.* (1991) used LWTs with surface station observations of atmospheric/rainwater chemistry data. Leśniok *et al.* (2010) used the Niedzweidz's Manual Classification, similar to the LWTs, to study the influence of synoptic regimes on surface $NO_2$ in Upper Silesia, Poland. They found that anticyclonic (cyclonic) conditions enhance (reduce) $NO_2$ concentrations increasing (reducing) pollution limit exceedances.

O'Hare and Wilby (1995) and Demuzere *et al.* (2009) investigated LWTs and rural surface ozone observations in the UK and the Netherlands, respectively. Anticyclonic conditions, through primary pollutant accumulation, were found to enhance surface ozone concentrations. However, cyclonic-induced tropospheric folding enhances free troposphere ozone incursion resulting in peak UK surface ozone concentrations.

Other studies have looked at the connection between meteorology and $NO_2$ tropospheric columns. Beirle *et al.* (2011) used Ozone Monitoring Instrument (OMI) column $NO_2$ and wind forecasts (below 500m) to analyse $NO_2$ transport from the isolated megacity Riyadh, Saudi Arabia, detecting leeward $NO_2$ plume transport. Hayn *et al.* (2009) performed a similar analysis of wind direction and column $NO_2$ over Johannesburg, South Africa. Zhou *et al.* (2012) found significant impacts of wind speed and precipitation on OMI column $NO_2$ over western Europe. Savage *et al.* (2008) investigated the interannual variability (IAV) of satellite $NO_2$ columns over Europe finding that meteorology influences $NO_2$ IAV more than emissions.

van der A *et al.* (2008) used GOME and SCIAMACHY data, 1996–2006, to look at column $NO_2$ seasonal patterns and trends. Over Europe, the peak industrial column $NO_2$ occurs during winter. They infer that reduced photolysis (increased $NO_2$ lifetime), not increased $NO_x$ emissions, is the main cause. The UK is the exception as the meteorological variability leads to peak $NO_2$ columns in July. However, Zhou *et al.* (2012) find that days with peak column $NO_2$ over the UK are in spring.

To our knowledge, LWTs have not previously been used to investigate synoptic patterns in fields of satellite observations of atmospheric chemistry. The aim of this paper is to investigate the influence of the UK surface

circulation patterns on atmospheric trace gas distributions by using the LWTs in order to classify distributions of satellite tropospheric $NO_2$ under these weather regimes.

## 2. Data

### 2.1. Lamb weather types

LWTs were originally derived using a manual method of classifying the atmospheric circulation patterns (mostly using sea level pressure) according to the wind direction and circulation type over the UK (Lamb 1972). Jenkinson and Collison (1977) created an automated classification scheme based on the mean sea level pressure at 16 points over western Europe (centred in the UK). From the pressure field at these points, the direction, strength and vorticity of the mean flow over the UK are calculated. Each day is then assigned both a vorticity type and a wind flow direction. Three vorticity types are used (neutral vorticity, cyclonic and anticyclonic) and eight wind flow directions (N, NE, E, SE, S, SW, W and NW) unless the flow vorticity is much stronger than the flow strength, when the day is classified solely as cyclonic or anticyclonic. There is also an unclassified LWT. Table I summarizes the LWT codes. For more details of the classification scheme, see Jones *et al.* (2013).

In this study, we use the dataset of Jones *et al.* (2013) which extends the objective LWT dataset by using daily midday (12:00 UT) grid-point mean sea level pressure data from NCEP/NCAR reanalysis (Kalnay *et al.*, 1996). We obtained the data from the Climatic Research Unit (CRU) at the University of East Anglia (www.cru.uea.ac.uk/cru/data/lwt/).

It would likely prove difficult to find statistically significant associations between the column $NO_2$ patterns and each individual LWT because their occurrence probability is too low. Therefore, we merged the LWTs into 11 classes, similar to O'Hare and Wilby (1995) and Tang *et al.* (2011), to increase the amount of data in each category (Table I). There are three synoptic classes: neutral vorticity (LWTs 11–18); cyclonic (20–28) and anticyclonic (0–8). There are eight flow directions: NE, E, SE, NW, W, SW, N and S (e.g. the south-westerly type is a combination of LWTs 5, 15 and 25). It should be noted that there is only one LWT definition per day, but each day is included in two of our weather classes (unless it is unclassified or are LWTs 0 or 20 as they have no flow direction), e.g. LWT 27 is in the cyclonic and north-westerly groups.

For the 7-year (2556-day) period 2005–2011, the percentage occurrence was calculated for each of the 11 classes. The relative occurrence of the synoptic conditions was: neutral vorticity 38.9%; cyclonic 26.1% and anticyclonic 33.7%. The most frequent wind flow directions were the W and SW directions at 16.7 and 14.4%, respectively.

**Table I.** The shaded region shows the 27 basic Lamb weather types with their number coding.[a]

| This Work | Anticyclonic | Neutral Vorticity | Cyclonic |
|---|---|---|---|
| | 0 A | | 20 C |
| **North-easterly** | 1 ANE | 11 NE | 21 CNE |
| **Easterly** | 2 AE | 12 E | 22 CE |
| **South-easterly** | 3 ASE | 13 SE | 23 CSE |
| **Southerly** | 4 AS | 14 S | 24 CS |
| **South-westerly** | 5 ASW | 15 SW | 25 CSW |
| **Westerly** | 6 AW | 16 W | 26 CW |
| **North-westerly** | 7 ANW | 17 NW | 27 CNW |
| **Northerly** | 8 AN | 18 N | 28 CN |

In this work these LWTs are grouped into three circulation types and eight wind directions, indicated in the outer row and column.
[a]LWTs also include −1 (unclassified) and −9 (non-existent day).

### 2.2. OMI $NO_2$ Tropospheric Column Data

OMI is mounted on NASA's EOS-Aura satellite and has an approximate London daytime overpass at 13:00 local time. It is a nadir viewing instrument with a pixel size of 312 $km^2$. We have taken the DOMINO tropospheric column $NO_2$ product, version 2.0, from the TEMIS (Tropospheric Emissions Monitoring Internet Service) website, http://www.temis.nl/airpollution/no2.html (Boersma *et al.*, 2011). We have binned $NO_2$ swath data from 1 January 2005 to 31 December 2011 onto a daily 13:00 0.25° × 0.25° grid between 43°–63°N and 20°W–20°E. All satellite retrievals have been quality controlled, and retrievals/pixels with cloud cover greater than 20% and poor quality data flags (flag = −1) were removed. The product uses the algorithm of Braak (2010) to identify OMI pixels affected by row anomalies and sets the data flags to −1. These are filtered out in this study. To obtain better spatial coverage, a time window for the OMI retrievals between 11:00 and 15:00 local time, was applied. Although the LWTs are based on meteorological reanalyses at 12:00 UT, we consider this temporal difference to be within an acceptable range.

## 3. Results

Composite maps of OMI tropospheric column $NO_2$ were derived for each of the 11 synoptic and wind direction classes for both winter (October to March) and summer (April to September). Figure 1 shows these composites for the cyclonic and anticyclonic conditions and Figure 2 shows the anomaly of each composite from the 7-year seasonal average. We focus primarily on the influences of cyclonic and anticyclonic weather patterns, as they have greater occurrence, and are therefore more statistically significant than the wind direction composites.

The summer and winter composites (Figure 1) show that $NO_2$ tropospheric column concentrations peak in the winter, as discussed by Tang *et al.* (2011), McGregor and Bamzelis (1995), Leśniok *et al.* (2010)

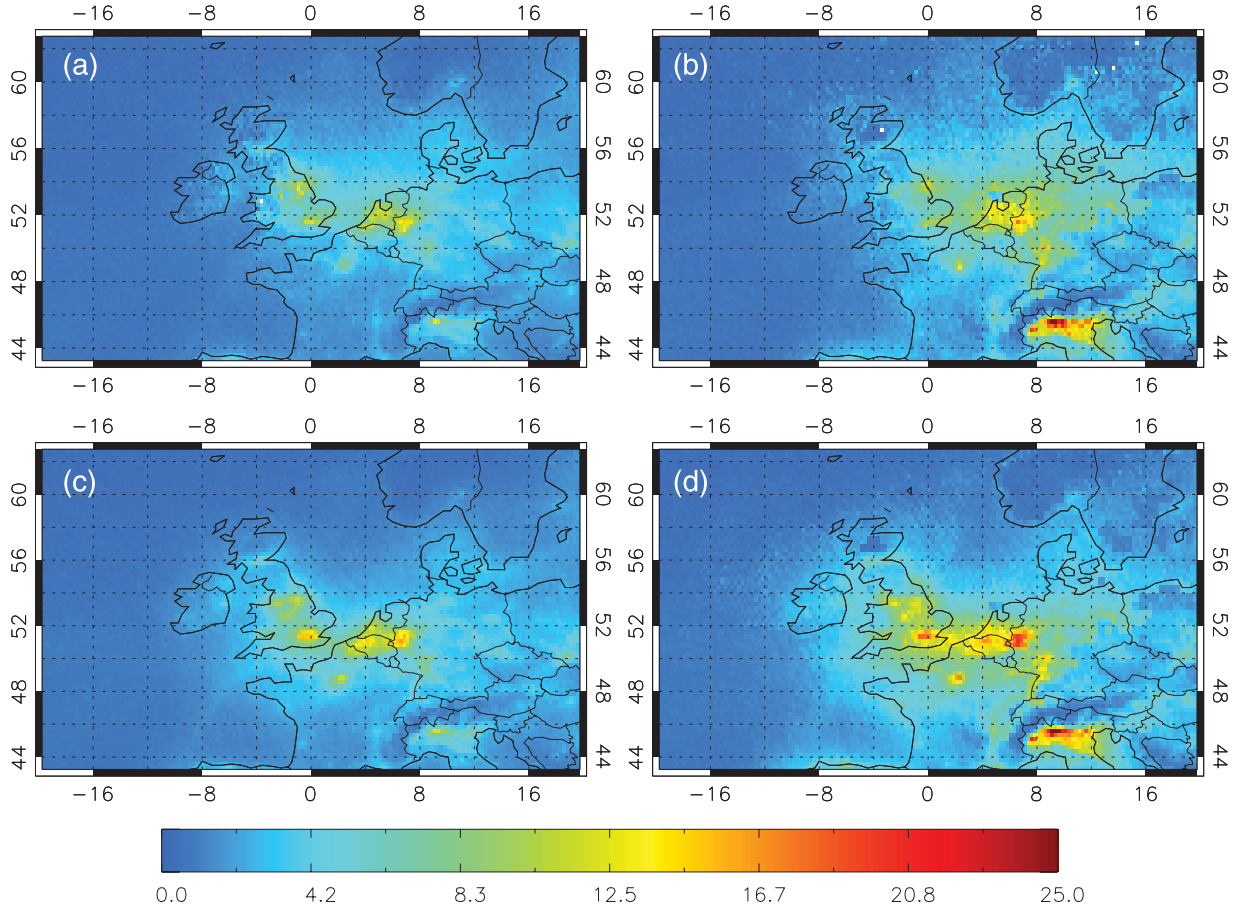


**Figure 1.** Composites of OMI column $NO_2$ ($\times 10^{15}$ molecules cm$^{-2}$) for (a) summer cyclonic, (b) winter cyclonic, (c) summer anticyclonic and (d) winter anticyclonic conditions.

and Demuzere *et al.* (2009). Winter conditions lead to greater emission of $NO_x$ from heat and electrical generating devices. The lower abundance of OH and slower photochemical processes also decrease the loss rate of $NO_2$. Over the Netherlands source regions, under cyclonic conditions, the peak $NO_2$ columns are $13 \times 10^{15}$molecules cm$^{-2}$ in summer and $13–16 \times 10^{15}$molecules cm$^{-2}$ in winter. Over the UK source regions, the peak UK cyclonic column $NO_2$ is approximately $13 \times 10^{15}$molecules cm$^{-2}$ in summer, while only $10 \times 10^{15}$molecules cm$^{-2}$ in winter. There is a less pronounced seasonality in the UK column $NO_2$ owing to the meteorological variability decreasing loss processes (e.g. photolysis), which are more active over continental Europe in summer. Under anticyclonic conditions, over the UK and the Netherlands source regions the summer peak is $16 \times 10^{15}$molecules cm$^{-2}$, while in winter the $NO_2$ concentrations reach $20 \times 10^{15}$molecules cm$^{-2}$.

McGregor and Bamzelis (1995) and Leśniok *et al.* (2010) noted that air mass stability (instability) under anticyclonic (cyclonic) conditions leads to reduced (increased) transport of $NO_2$ from sources. This is seen in Figure 1, where the $NO_2$ concentrations are higher under anticyclonic conditions. In winter, the $NO_2$ concentrations over South East England and the Netherlands range from $10–16 \times 10^{15}$molecules cm$^{-2}$ to $16–20 \times 10^{15}$molecules cm$^{-2}$ in cyclonic and anticyclonic conditions, respectively. The same occurs in summer, but with lower $NO_2$ concentrations at $13 \times 10^{15}$ (cyclonic) and $16 \times 10^{15}$ molecules cm$^{-2}$ (anticyclonic).

To quantify the differences between the synoptic regimes, we subtracted the 7-year seasonal average (of all weather types) from the winter and summer cyclonic and anticyclonic composites (Figure 2). We use the Wilcoxon rank test (WRT) to examine the significance of the differences, at the 5% significance level ($p < 0.05$), in the composite-total period averages. The WRT is the nonparametric counterpart of the Student *T*-test and so relaxes the constraint on normality of the underlying distributions (Pirovano *et al.*, 2012). In Figure 2, areas where the anomalies are significant are outlined with black polygons. In the cyclonic case, a significant positive-negative dipole exists, with negative anomalies over the southern UK and positive anomalies over the North Sea. The higher winter $NO_2$ concentrations lead to an intense dipole, with maximum positive anomalies greater than $5 \times 10^{15}$ molecules cm$^{-2}$ and the lowest negative anomalies less than $-5 \times 10^{15}$ molecules cm$^{-2}$. In summer, these anomalies peak at similar values but their spatial extent is much less. Potential reasons why the area of the anomaly is reduced in summer include both the more rapid removal

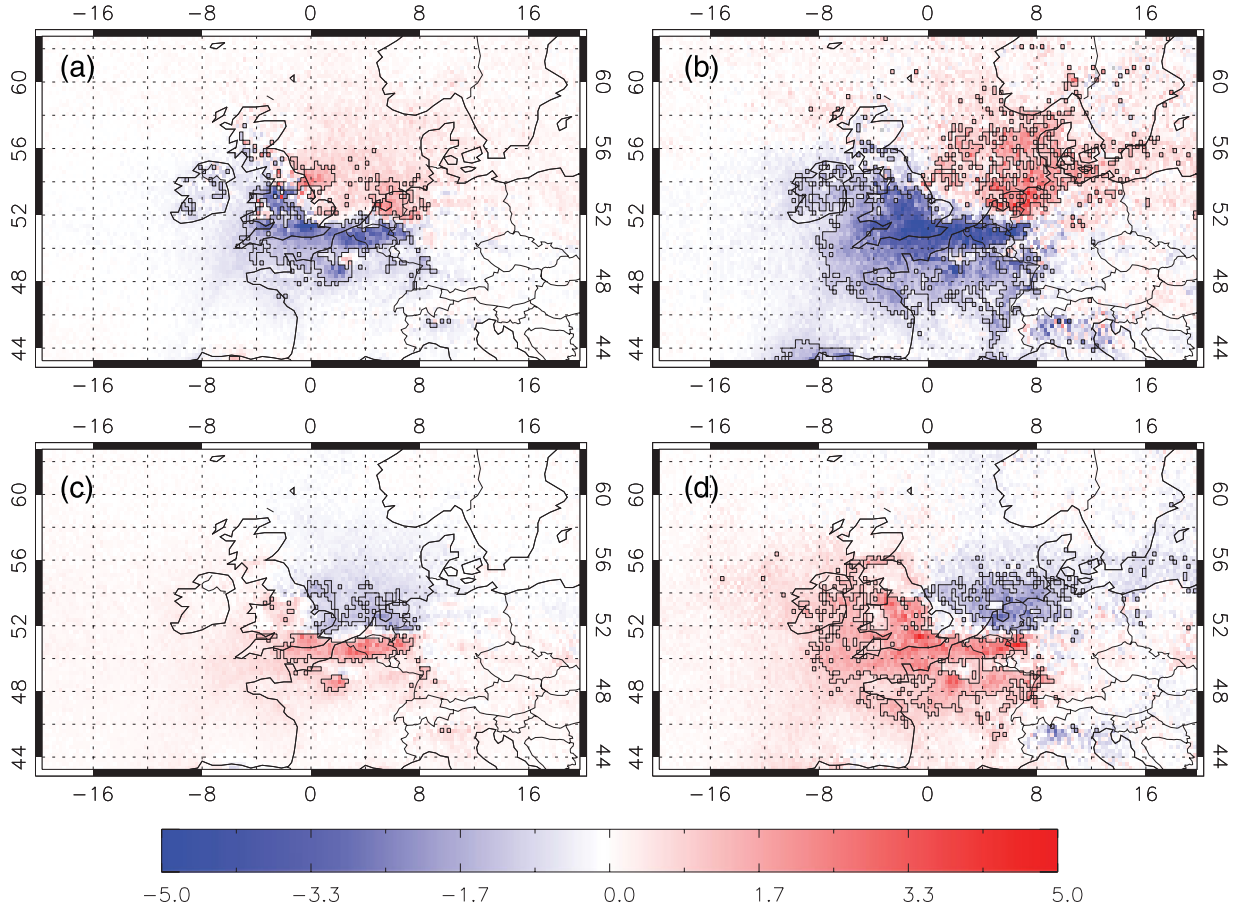


**Figure 2.** Anomalies of OMI column $NO_2$ composites compared to seasonal 7-year average ($\times 10^{15}$ molecules $cm^{-2}$) for (a) summer cyclonic, (b) winter cyclonic, (c) summer anticyclonic and (d) winter anticyclonic conditions. Black boxes indicate where the anomalies are statistically significant at the 5% level.

of $NO_2$ giving less accumulation under stagnant conditions and lighter winds in the summer causing slower transport from source regions. Typically, cyclonic conditions are indicative of westerly and south-westerly flow. Therefore, the anomalies potentially reveal transport of $NO_2$ off the UK mainland into the North Sea. In the more stable anticyclonic conditions, the inverse of the cyclonic anomaly dipole exists with positive anomalies, $4–5 \times 10^{15}$ molecules $cm^{-2}$, over the UK and negative anomalies, $-3 \times 10^{15}$ molecules $cm^{-2}$, over the North Sea. This occurs for both seasons, but with larger spatial patterns in winter. It is probable that the anomaly pattern occurs as less $NO_2$ is transported out to the North Sea and more remains over the UK.

We averaged all OMI pixels within 6°W – 2°E and 59° – 50°N (Figure 1) to form a UK-average time series. Figure 3(a) and (b) shows the mean annual cycles and their anomalies for the three synoptic classes. The anticyclonic column $NO_2$ seasonal cycle is well pronounced with maximum (minimum) winter (summer) concentrations of approximately 7 (3) $\times 10^{15}$ molecules $cm^{-2}$. The cyclonic column $NO_2$ cycle is less pronounced with similar concentrations in summer and winter of approximately 3 – 4 $\times 10^{15}$ molecules $cm^{-2}$. The neutral conditions show a seasonal pattern between the cyclonic and anticyclonic conditions. Figure 3(c)–(e) shows the correlation of the UK monthly mean columns with their standard deviations. The scattered points all sit above the 1 : 1 line showing that the monthly mean values are always greater than their temporal variability. Figure 3(d) and (e) also emphasizes the larger range of mean column $NO_2$ under anticyclonic conditions compared with cyclonic conditions. Overall, the largest relative differences are in winter, likely owing to a combination of more intense winter cyclonic and anticyclonic dynamics and reduced photochemical processes. In winter, increased poleward momentum flux results in larger atmospheric instabilities. Therefore, the more intense cyclones further reduce column $NO_2$ above source regions in winter. However, winter anticyclones are associated with cold denser air masses enhancing atmospheric blocking and prolonged stable conditions, therefore, accumulating $NO_2$ more efficiently. Photochemically, under anticyclonic conditions, in summer stronger photolysis converts more $NO_2$ to NO, but in winter reduced solar intensity and cloudier conditions limit $NO_2$ to NO conversion. The neutral vorticity conditions typically have similar concentrations to the cyclonic conditions in summer and anticyclonic conditions in winter over the study period.

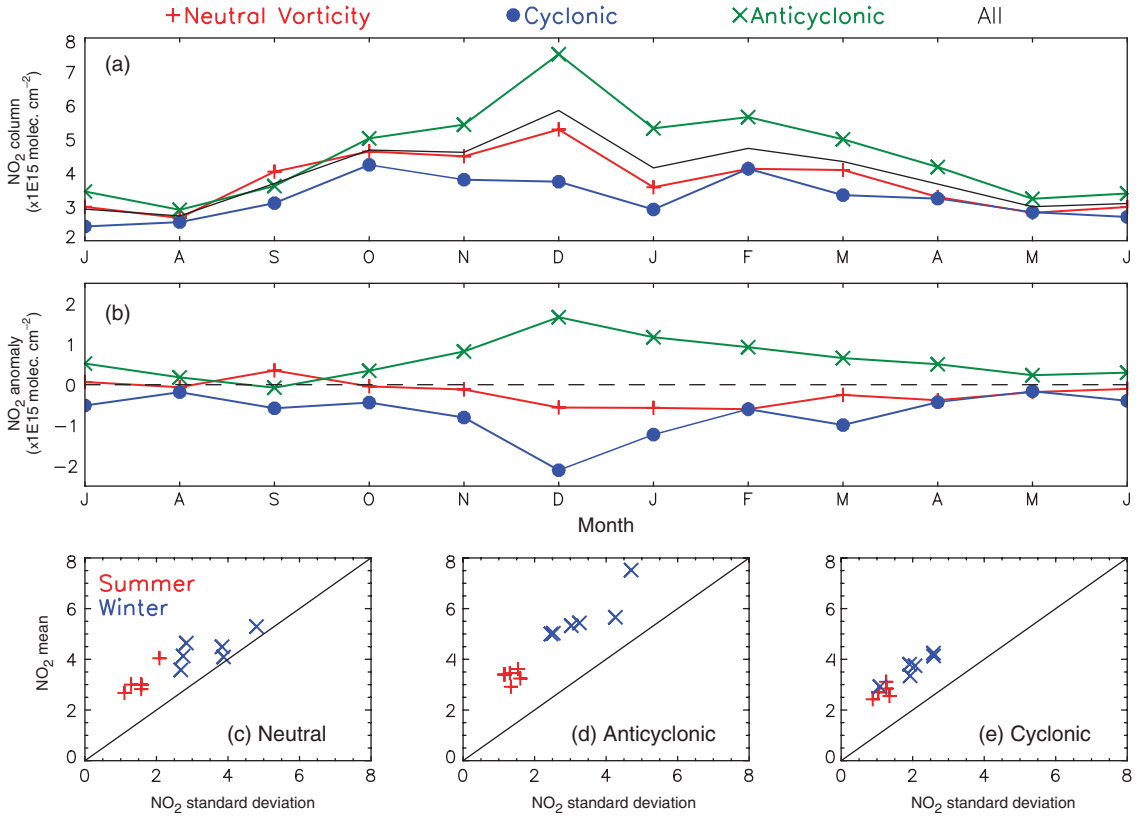


**Figure 3.** OMI $NO_2$ columns ($x10^{15}$ molecules $cm^{-2}$) averaged over the UK (see text) under neutral vorticity, cyclonic and anticyclonic conditions for (a) mean annual cycle of monthly means, including black line for all conditions, and (b) anomaly of monthly means with respect to all conditions. Panels (c)–(e) show the correlation of the monthly means with their standard deviations.

We also find that the influence of the wind directions on the OMI $NO_2$ fields can be significant. Note that owing to the lower frequency of each of the eight wind directions, these are not seasonal composites but use all seven years of data regardless of season. Two examples of the wind-induced $NO_2$ transport are shown in Figure 4. Figure 4(a) shows south-easterly flow off continental Europe, where $NO_2$ (up to $20 \times 10^{15}$molecules $cm^{-2}$) is transported away from London and Lancashire towards the Midlands and the Irish Sea, respectively. In Figure 4(b), the south-westerly flow is transporting $NO_2$ (up to $13 \times 10^{15}$molecules $cm^{-2}$) away from London and the M62 corridor out into the North Sea. The transport impact from the south-easterly flow is much greater, but because these classes can contain different proportions of each vorticity type, this might account for the greater transport when compared with the south-westerly flow. Figures 4(c) and (d) show the anomalies in $NO_2$ for these two flow directions with respect to the 7-year OMI average. The significant positive anomalies suggest that south-easterly flow is transporting up to $5 \times 10^{15}$molecules $cm^{-2}$ away from the source regions. In Figure 4(d), positive (negative) anomalies, over (under) $+(-)$ $5 \times 10^{15}$molecules $cm^{-2}$ show where the south-westerly flow has transported $NO_2$ away from the source regions out into the North Sea.

Finally, we have also investigated the link between the winter North Atlantic Oscillation (NAO) and column $NO_2$ data using the NAO index from CRU (Jones *et al.*, 1997; available from www.cru.uea.ac.uk/cru/data/nao). However, we could not find any significant spatial differences in the $NO_2$ columns between the positive and negative NAO phases.

## 4. Conclusions

We have shown that the quality of the OMI $NO_2$ tropospheric column product is good enough to detect the influences of synoptic meteorology on $NO_2$ tropospheric columns over the UK. UK column $NO_2$ peaks in winter (October to March) under anticyclonic conditions. It is likely that increased winter $NO_x$ emissions from energy generation coupled with more stable conditions and reduced photolysis allow for the accumulation of $NO_2$ above the source regions. The cyclonic conditions have a less-defined seasonal pattern, but column $NO_2$ over the UK source regions is slightly higher in summer (April to September). This is consistent with more intense winter cyclonic conditions, which reduce column $NO_2$ concentrations and has more impact than $NO_2$ loss in summer from enhanced photolysis. The influence of transport of $NO_2$ by wind flow directions can also be seen in the OMI $NO_2$ data, with good

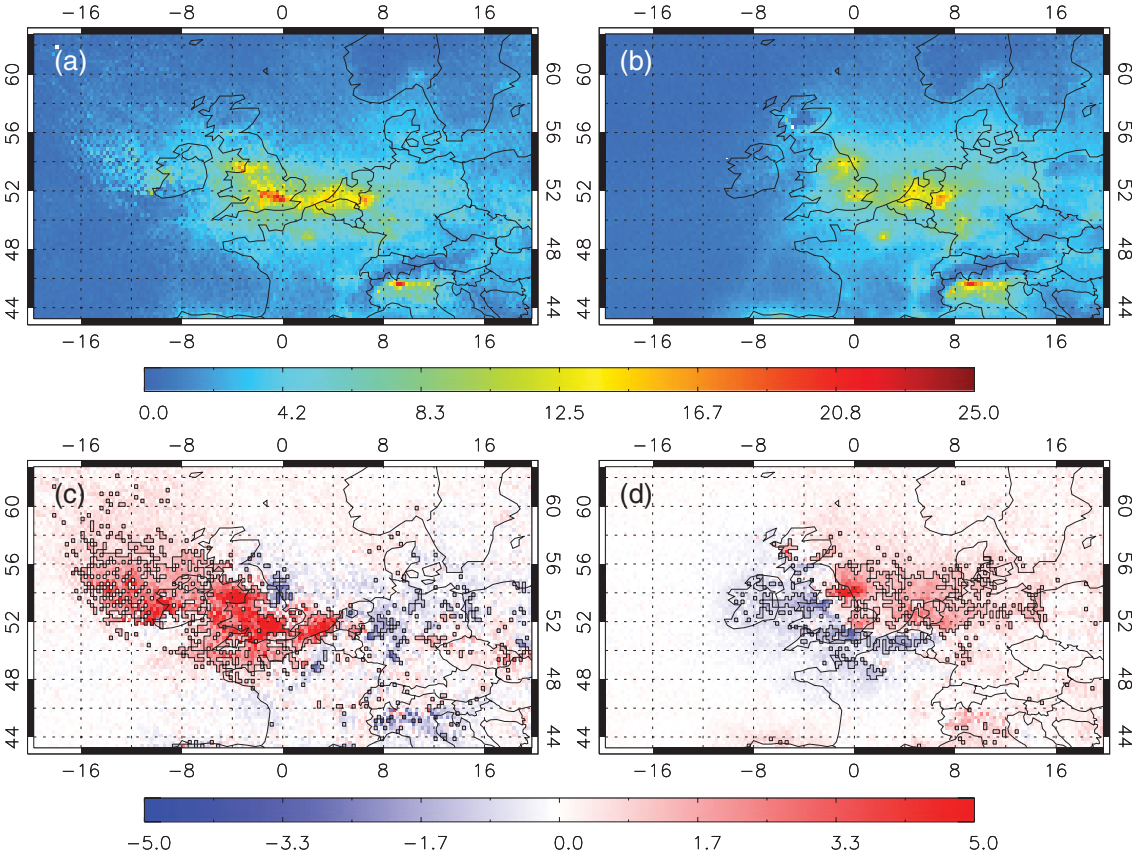


**Figure 4.** Composites of OMI column $NO_2$ ($\times 10^{15}$ molecules $cm^{-2}$) under different wind flow directions and difference of these with respect to 7-year average. (a) South-easterly flow, (b) south-westerly flow, (c) south-easterly difference and (d) south-westerly difference.

examples being the south-easterly and south-westerly flow directions. The spatial patterns in the $NO_2$ fields associated with these transport regimes are significantly different at a 5% confidence level using the Wilcoxon rank test.

These statistically significant meteorology–atmospheric chemistry relationships, seen by OMI, can potentially be used as a model validation tool. This dataset will allow progress beyond simply using the satellite data for operational model validation (calculation of means and biases, see Dennis *et al.* (2010)) and can be used to test the model's ability in order to reproduce the influence of meteorology on $NO_2$ (dynamic model evaluation). For chemistry-climate models this can also be used to evaluate the model under each of the synoptic regimes, rather than just using averages over seven or so years. For further work, we plan to test these same relationships in the Met Office Air Quality in the Unified Model (AQUM) (Savage *et al.*, 2013) and further investigate the processes controlling the LWT–$NO_2$ column relationships. In particular, we will explore the relative importance of transport processes versus difference in photochemistry between the classes.

## Acknowledgements

We acknowledge the use of OMI tropospheric $NO_2$ column data from www.temis.nl and LWT data from www.cru.uea.ac.uk. This work was supported by the NERC National Centre for Earth Observation (NCEO).

## References

Beirle S, Boersma BF, Platt U, Lawrence MG, Wagner T. 2011. Megacity emissions and lifetimes of nitrogen oxides probed from space. *Science* **333**: 1737.

Boersma KF, Eskes HJ, Dirksen RJ, van der A RJ, Veefkind JP, Stammes P, Huijnen V, Kleipool QL, Sneep M, Claas M, Claas J, Leitão J, Ritcher A, Zhou Y, Brunner D. 2011. An improved tropospheric $NO_2$ column retrieval algorithm for the ozone monitoring instrument. *Atmospheric Measurement Techniques* **4**: 1905–1928.

Braak R. 2010. Row Anomaly Flagging Rules Lookup Table. *KNMI Technical Document*, TN-OMIE-KNMI-950.

Davies TD, Dorling SR, Pierce CE. 1991. The meteorological control on the anthropogenic ion content of precipitation at three sites in the UK: the utility of Lamb weather types. *International Journal of Climatology* **11**: 795–907.

Demuzere M, Trigo RM, Vila-Guerau de Arellano J, van Lipzig NPM. 2009. The impact of weather and atmospheric circulation on O3 and PM10 levels at a rural mid-latitude site. *Atmospheric Chemistry and Physics* **9**: 2695–2714.

Dennis R, Fox T, Fuentes M, Gilliland A, Hanna S, Hogrefe C, Irwin J, Trivikrama Rao ST, Scheffe R, Schere K, Steyn D, Venkatramh A. 2010. A framework for evaluating regional-scale numerical photochemical modelling systems. *Environmental Fluid Mechanics* **10**: 471–489.

Hayn M, Beirle S, Hamprecht FA, Platt U, Menze BH, Wagner T. 2009. Analysing spatio-temporal patterns of the global $NO_2$-distribution retrieved from GOME satellite observations using a generalised additive model. *Atmospheric Chemistry and Physics* **9**: 6459–6477.

Huijnen V, Eskes HJ, Poupkou A, Eblern H, Boersma KF, Foret G, Sofiev M, Valdebnito A, Flemming J, Stein O, Gross A, Robertson L, D'Isidoro MD, Kioutsioukis I, Friese E, Amstrup B, Bergstrom R, Strunk A, Vira J, Zyryanov D, Melas D, Peuch VH, Zerefos C. 2010. Comparisons of OMI $NO_2$ tropospheric columns with an ensemble of global and European regional air quality models. *Atmospheric Chemistry and Physics* **110**: 3273–3296.

Jenkinson AF, Collison FP. 1977. An initial climatology of gales over the North Sea. Synoptic Branch Memorandum No. 62, Met Office, Exeter.

Jones PD, Jónsson T, Wheeler D. 1997. Extension to the North Atlantic Oscillation using early instrumental pressure observations from Gibraltar and South-West Iceland. *International Journal of Climatology* **17**: 1433–1450.

Jones PD, Harpham C, Briffa KR. 2013. Lamb weather types derived from reanalysis products. *International Journal of Climatology* **33**: 1129–1139.

Kalnay E, Kanamitsu M, Kistler R, Collins W, Deaven D, Gandin L, Iredell M, Saha S, White G, Wollen J, Zhu Y, Chelliah M, Ebisuzaki W, Higgins W, Janowiak J, Mo KC, Ropelewski C, Wang J, Leetmaa A, Reynolds R, Jenne R, Joseph D. 1996. The NCEP/NCAR 40 year reanalysis project. *Bulletin of the American Meteorological Society* **77**: 437–471.

Lamb HH. 1972. British Isles Weather types and a register of daily sequence of circulation patterns, 1861-1971. *Geophysical Memoir* 116, HMSO, London, 85.

Leśniok M, Małarzewski Ł, Niedźwiedź T. 2010. Classification of circulation types for Southern Poland with an application to air pollution concentrations in Upper Silesia. *Physics and Chemistry of the Earth* **35**: 516–522.

McGregor GR, Bamzelis D. 1995. Synoptic typing and its application to the investigation of weather air pollution relationships, Birmingham, United Kingdom. *Theoretical and Applied Climatology* **51**: 223–236.

O'Hare GP, Wilby R. 1995. A review of ozone pollution in the United Kingdom and Ireland with an analysis using Lamb weather types. *The Geographical Journal* **161**: 1–20.

Pirovano G, Balzarini A, Bessagnet B, Emery C, Kalos G, Meleux F, Mitsakou C, Nopmongcol U, Riva GM, Yarwood G. 2012. Investigating impacts of chemistry and transport model formulation on model performance at European scale. *Atmospheric Environment* **53**: 93–109.

Savage NH, Pyle JA, Braesicke P, Wittrock F, Richter A, Nüß H, Burrows JP, Schultz MG, Pulles T, van het Bolscher M. 2008. The sensitivity of Western European $NO_2$ columns to interannual variability of meteorology and emissions: a model-GOME study. *Atmospheric Science Letters* **9**: 182–188.

Savage NH, Agnew P, Davis LS, Ordóñez C, Thorpe R, Johnson CE, O'Connor MO, Dalvi M. 2013. Air quality modelling using the Met Office Unified Model (AQUM OS24-26): model description and initial evaluation. *Geoscientific Model Development* **6**: 353–372.

Tang L, Rayner D, Haeger-Eugensson M. 2011. Have meteorological conditions reduced $NO_2$ concentrations from local emission sources in Gothenburg? *Water Air Soil Pollution* **221**: 275–286.

van der A RJ, Eskes HJ, Boersma KF, van Noije TPC, Van Roozendael M, De Smedt I, Peters DHMU, Meijer EW. 2008. Trends, seasonal variability and dominant $NO_x$ sources derived from a ten year record of $NO_2$ measured from space. *Journal of Geophysical Research* **113**: 12 pp, DOI: 10.1029/2007JD009021.

Zhou Y, Brunner D, Hueglin C, Henne S, Staelhelin J. 2012. Changes in OMI tropospheric $NO_2$ columns over Europe from 2004 to 2009 and the influence of meteorological variability. *Atmospheric Environment* **46**: 482–495.

 